Perception, 2007, volume 36, pages 808 – 820

DOI:10.1068/p5610c

BOLD activation varies parametrically with corner angle throughout human retinotopic cortex

Xoana G Troncoso¶‡, Peter U Tse§, Stephen L Macknik¶, Gideon P Caplovitz§, Po-Jang Hsieh§, Alexander A Schlegel¶, Jorge Otero-Millan¶, Susana Martinez-Conde¶#

¶ Department of Neurobiology, Barrow Neurological Institute, 350 West Thomas Road, Phoenix, AZ 85013, USA; e-mail: smart@neuralcorrelate.com; § HB 6207, Moore Hall Department of Psychological and Brain Sciences, Dartmouth College Hanover, NH 03755, USA; ‡ Gatsby Computational Neuroscience Unit, University College London, 17 Queen Square, London WC1N 3AR, UK

Received 1 April 2006, in revised form 20 September 2006; published online 25 May 2007

Abstract. The Alternating Brightness Star (ABS) is an illusion that provides insight into the relationship between brightness perception and corner angle. Recent psychophysical studies of this illusion have shown that corner salience varies parametrically with corner angle, with sharp angles leading to strong illusory percepts and shallow angles leading to weak percepts. It is hypothesized that the illusory effects arise because of an interaction between surface corners and the shape of visual receptive fields: sharp surface corners may create hotspots of high local contrast due to processing by center – surround and other early receptive fields. If this hypothesis is correct, early visual neurons should respond powerfully to sharp corners and curved portions of surface edges. Indeed, the primary role of early visual neurons may be to localize the discontinuities along the edges of surfaces. If so, all early visual areas should show greater BOLD responses to sharp corners than to shallow corners. On the other hand, if corner processing is exclusively constrained to certain areas of the brain, only those specific areas will show greater responses to sharp vs shallow corners. To address this we explored the BOLD correlates of the ABS illusion in the human visual cortex using fMRI. We found that BOLD signal varies parametrically with corner angle throughout the visual cortex, offering the first neurophysiological correlates of the ABS illusion. This finding provides a neurophysiological basis for the previously reported psychophysical data that showed that corner salience varied parametrically with corner angle. We propose that all early visual areas localize discontinuities along the edges of surfaces, and that specific cortical corner-processing circuits further establish the specific nature of those discontinuities, such as their orientation.

1 Introduction

The Alternating Brightness Star (ABS) is a recently described brightness illusion (Martinez-Conde and Macknik 2001; Troncoso et al 2005) related to Vasarely's classic 'nested squares' (Vasarely 1970; Hurvich 1981) (figure 1). Vasarely's 'nested squares' show that 90° corners in a luminance gradient appear as more salient than adjacent edges (ie non-corners) of the same luminance. The ABS illusion (figure 2) further shows a corner angle brightness reversal (CABR) effect, where the illusory folds in a corner gradient appear dark or bright depending on the polarity of the angle (concave or convex) and the direction of the gradient (black-to-white or white-to-black). The ABS illusion also makes evident a corner angle salience variation (CASV) effect, where the perceived salience of corners in a luminance gradient depends on the corner angle, with sharp corners appearing more salient than shallow corners (for an interactive demo of the ABS illusion visit http://smc.neuralcorrelate.com/demos/ABS-illusion.html).

The CABR and CASV effects cannot be explained by the physical luminance of the stimuli (figure 2e), or by optical blurring due to the physical limitations of the eye (figure 2f), but are best explained by changes in local contrast (figures 2d and 2g). In fact, when the ABS is blurred with a Gaussian filter, the result is opposite to our perception of the illusion. However, when the ABS is filtered with a difference of Gaussians (DOG) filter (ie to simulate the responses of center – surround receptive fields)

Author to whom correspondence should be addressed.

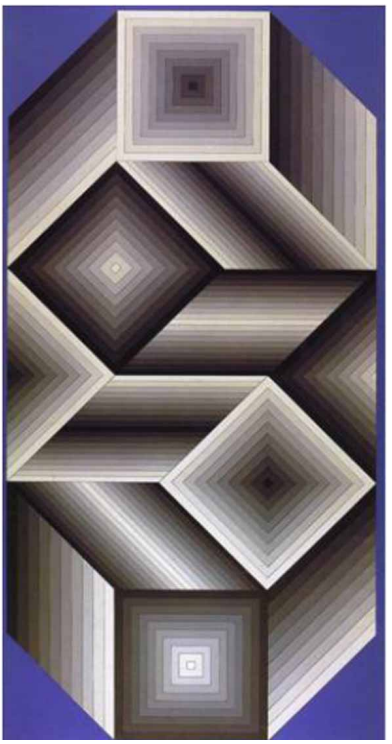

Figure 1. Vasarely's *Utem* (1981). Reproduced, with permission by the Vasarely Foundation, from (Vasarely 1982). Note the four sets of nested squares. The two nested squares of decreasing luminance (from the center to the outside) have bright illusory diagonals. The two nested squares of increasing luminance (from the center to the outside) have dark illusory diagonals. The physical luminance of each individual square remains constant at all points; however, the corners of the squares appear perceptually more salient than the straight edges, forming illusory X-shapes that seem to irradiate from the very center of each set of squares.

the output qualitatively matches our perception of the illusion (figures 2d and 2g; see also Troncoso et al 2005).

Recent psychophysical measurements of the ABS illusion reveal a parametric relationship between corner salience and corner angle, and suggest that the increase in local perceived brightness at corners, curves, and other discontinuities is due to the interaction between the shape of corners and the shape of early visual receptive fields (Troncoso et al 2005).

Previous models suggest a primary role of specific extrastriate circuits in corner perception and processing (Hubel and Wiesel 1965; Pasupathy and Connor 1999; Ito and Komatsu 2004). Here, we propose that most (possibly all) early visual receptive fields, cortical and subcortical, may be equipped to locate corners on surfaces and to encode the sharpness of their angle. In this model, more specialized corner-processing circuits, such as those found in V4 (Pasupathy and Connor 1999), may encode specific features about corners, such as their orientation or their relative placement within a global contour or shape. If our hypothesis is correct, then all localized retinotopic areas in the occipital lobe will respond in a parametric way to corners of varying angles. If our hypothesis is incorrect, only those areas that are classically concerned with corner processing will be activated in a differential manner with corner angle.

No previous studies of corner processing have been conducted on humans with whole-brain fMRI imaging. The goal of the present study is to determine the neural substrates of the ABS illusion, particularly the CASV effect, in the visual cortex of human subjects. We presented normal volunteers with ABSs having equivalent angles to those used previously in psychophysical experiments (Troncoso et al 2005), while acquiring fMRI data. We localized the retinotopic cortical regions that modulated their activity in correlation with the angle of the corner. The BOLD signal correlates of the ABS illusion matched the psychophysical results: BOLD signal responses were stronger for sharp angles than for shallow angles. A parametric relationship between corner

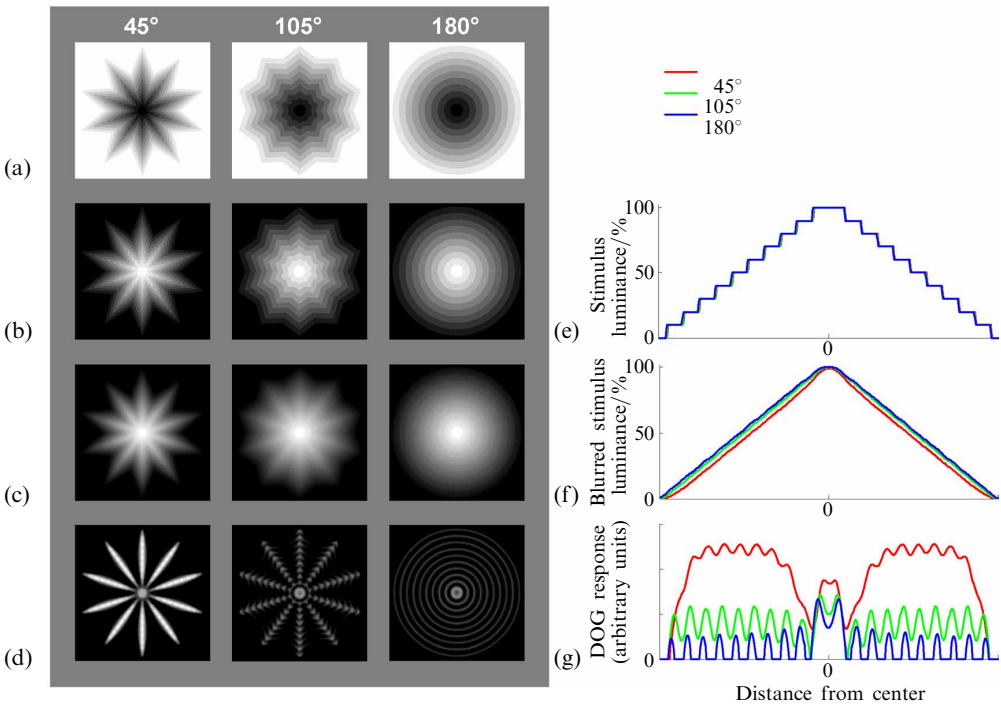

Figure 2. The ABS illusion (Martinez-Conde and Macknik 2001; Troncoso et al 2005) [(a) and (b)]. The stimuli are made of concentric stars of graded luminance. The gradient from the center to the outside of each set of stars has 10 luminance steps. In (a) the innermost star is black; the outermost star is white. In (b) the innermost star is white; the outermost star is black. The illusory folds that radiate from the center of each set of stars appear light or dark depending on the polarity of the corner angle and the direction of the luminance gradient (corner angle brightness reversal effect). However, all illusory folds are physically equal to each other in luminance. Note also that the strength of the illusory foldss depends on the sharpness of the corner angle (corner angle salience variation effect). Sharp corner angles (45° column) result in stronger illusory folds. Shallow corner angles produce weaker (105° column) or no (180° column) illusory folds. (c) Blurred version of the stars in (b) (Gaussian filtering). (d) Result of filtering the stimuli in (b) with a difference of Gaussians (DOG) filter, simulating the output of center – surround receptive fields. (e) Luminance profile along one of the arms of the star for the stimuli in (b). The illusory folds have the same physical luminance in the three angle conditions (the three lines overlap). (f) Luminance profile along one of the arms of the star for the stimuli in (c). The illusory folds cannot be explained by blurring: blurring causes sharp corners to have lower luminance than shallow corners, contrary to our perception of the illusion. (g) Luminance profile along one of the arms of the star for the stimuli in (d). The center – surround simulation qualitatively matches our perception of the illusion: the predicted response is highest for the sharpest corner angle, and decreases as the corner angle becomes shallower.

angle and strength of BOLD signal was moreover observed in all individual retinotopic areas, and with similar magnitudes. This suggests that corner and angle processing are generalized properties of the early visual system, and not solely the function of a small subset of extrastriate circuits. Therefore we propose that specific corner-processing circuits, such as end-stopped cells in extrastriate areas (Hubel and Wiesel 1965), as well as corner-processing neurons in area V4 (Pasupathy and Connor 1999), serve to determine precise characteristics of corners, such as their orientation, and their particular relationship to other stimulus features and surface attributes. These results offer insights into the neural mechanisms responsible for corner processing, and also provide new data regarding the stage of the visual hierarchy in which corner processing may arise.

2 Methods

2.1 *Subjects*

Twenty-four healthy volunteers (of both genders between the ages of 18 and 40 years) participated in the study. Subjects gave written, informed consent according to the guidelines of the Dartmouth College's Institutional Review Board (protocol number 15782) and were paid $20 per session. All subjects were scanned on (at least) two separate days, with one session per day (one session for retinotopic mapping and one or two sessions to measure BOLD responses under the different experimental conditions).

2.2 *Stimuli*

Visual stimuli were generated with custom MATLAB code. ABSs were drawn as nested star-shaped polygons. The luminance of the nested polygon was incremented (or decremented) in a linear gradient from the center to the periphery of each ABS, including the 180° ABS. All ABSs tested (inside red rectangles, figure 3, column A) were identical in size and extended across the monitor screen (figure 3, column B). ABSs were counterphase-flickered (between figure 3, columns B and C) at 2 Hz. Flickering the stimuli in this way had the dual benefit of counteracting luminance adaptation and maximizing the stimulation of the visual system. Stimuli were projected onto a Plexiglass™ screen outside the bore of the magnet, and viewed via a tangent mirror inside the magnet that permitted a maximum of 22 deg × 16 deg visible area. The projected image was smaller than this area and subtended approximately 17 deg × 12 deg. The luminance of the monitor was linearized. All ABSs had the same number of arms or vertices ($n = 20$). To control for the potential effects of global luminance changes across conditions, we normalized the overall spatial luminance of each ABS with respect to the 180° condition. After luminance normalization, global luminance contrast (distance from the image-luminance peak to the image-luminance trough) was roughly equivalent in all conditions, with the highest contrast in the 180° ABS, and lowest contrast in the 15° ABS. This was a conservative control, as it was designed to work against our hypothesis that BOLD signal should increase with corner-angle sharpness.

2.3 *Design*

Continuous whole-brain BOLD signal was acquired at the Dartmouth Brain Imaging Center on a GE 1.5 T sigma scanner with a head coil. We collected standard T2*-weighted echoplanar functional images using 25 slices (4.5 mm thick with 3.75 mm × 3.75 mm in-plane voxel resolution; inter-slice distance 1 mm, TR = 2500 ms, flip angle = 90°, field of view = 240 mm × 240 mm × 256 mm, descending interleaved slice acquisition, matrix size = 64 × 64) oriented approximately along the anterior-commissure posterior-commissure plane. These slices were sufficient to encompass the entire brain of each subject. Cushions were used to minimize head motion. A T1-weighted anatomical image with the same slice orientation as the EPI was collected for each subject, as was a T2-weighted high-resolution anatomical scan. T1-weighted anatomical images were acquired with a high-resolution 3-D spoiled gradient-recovery sequence (SPGR; 124 sagital slices, TE = 6 ms, TR = 25 ms, flip angle = 25°, 1 mm × 1 mm × 1.2 mm voxels) as well as a T1-weighted coplanar anatomical image with the same slice orientation as the EPI data which were used for co-registration.

The experiment had a standard fMRI block design, with 11 (5 ABS condition and 6 fixation) 20 s blocks. Each run began with 10 s of dummy scans (four volumes, which were discarded) to bring spins to baseline. Each run thus lasted a total of 230 s. Condition order was randomized on each run. Subjects carried out a minimum of 10 runs each, and a maximum of 24. The first and last blocks were always fixation-only, and condition blocks were always separated by a fixation-only block. An entire cortical volume was scanned 8 times per 20 s block (each block consisted of 40 cycles of the stimulus counterphase flickering at 2 Hz).

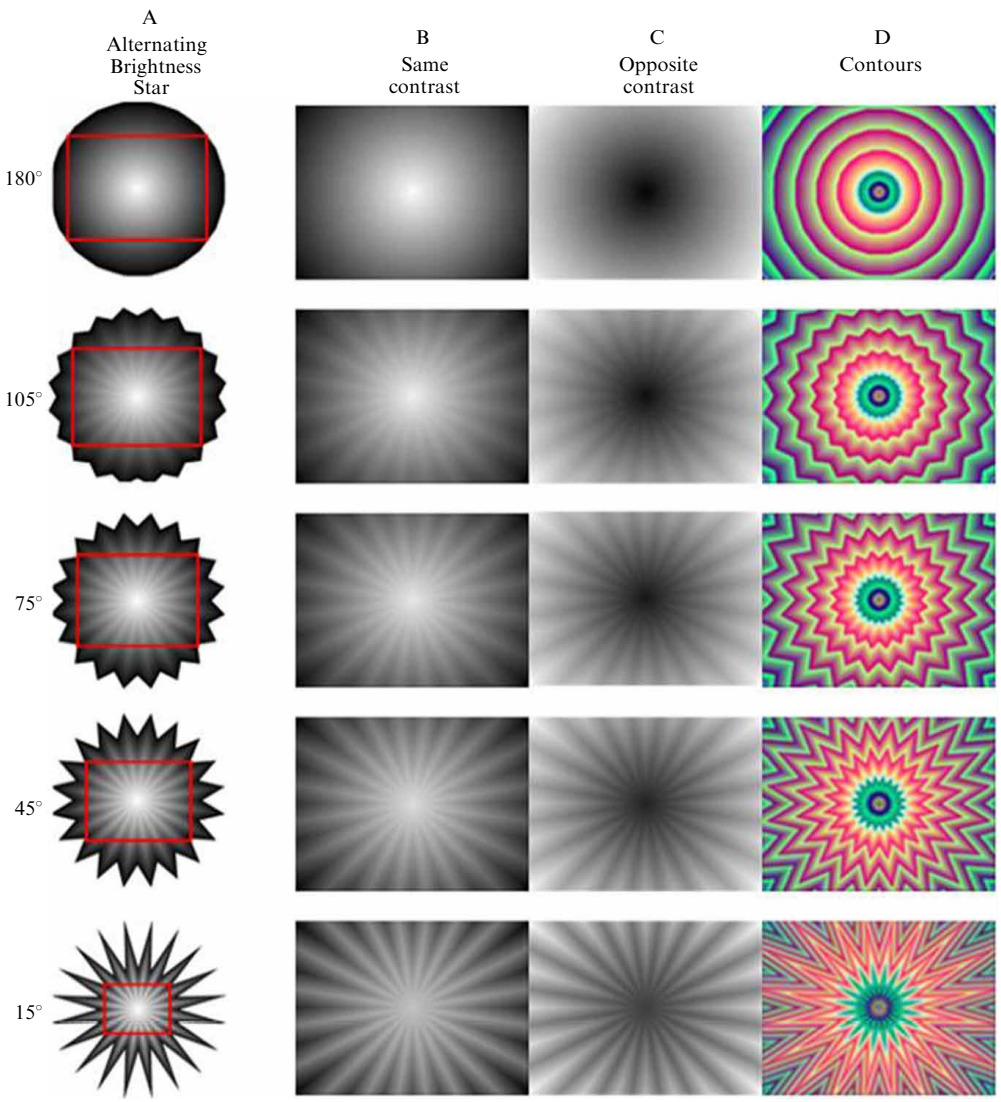

Figure 3. ABS stimuli used during the experiment. Column A: ABSs with different vertex angles. As the protruding vertices become sharper (lower rows), the brightness/salience effect grows stronger. Thus the peaks and troughs of each arm of the star look more salient with sharper angles, despite the fact that they have the same luminances as in lower angles. The (red) rectangle over each ABS represents the part of the stimulus that was cropped and scaled to create the stimuli in columns B, C, and D. Column B: same stimulus as in column A, now zoomed in and normalized for overall luminance. The illusory effect remains stronger for the lower rows, which have sharper angles, even though their maximal overall contrast is lower than in the upper rows (due to the luminance normalization). Column C: same as column B, but now sign-reversed. Column D: same as in columns B – C, but now with a randomized color gradient. All stimuli presented during the experiment were from columns B and C.

We controlled for eye movements, alertness, and attention to the fovea by requiring subjects to perform a demanding reaction-time task, in which the subject had to respond (via button press) to randomly occurring changes in the color of the fixation point. The fixation point was approximately 0.2 deg $\times$ 0.2 deg and changed color on average about once every 1.5 s. This color change occurred an equal number of times during each block.

Changes in fixation color—and the resultant button presses—were evenly distributed across the experimental conditions. This task could be carried out successfully only if the subject was fixating during both condition and fixation-only blocks, and attending to the fixation point carefully. Subjects were required to perform at 92.5% correct or better during each run or the run was not analyzed further. Thus subjects were only permitted an average of one miss or delayed response per block.

2.3.1 *Data preprocessing.* Data were analyzed offline using Brain Voyager (BV) 4.9.6 and custom MATLAB software. Effects of small head movements were removed with BV's motion-correction algorithm. Slice scan-time correction was carried out to correct for the fact that slices were not collected at the same time. Slices were corrected to have the same mean intensity. Functional data were not smoothed in the space domain, but any low-frequency temporal fluctuations whose temporal wavelength was greater than 29 TRs were removed. These preprocessing stages did not introduce correlations between a voxel and its neighbors. For each subject, the functional data were co-registered to the high-resolution anatomical image and normalized into the Talairach stereotactic coordinate space, which enables comparisons to be made across subjects.

Retinotopy (figure 4) was carried out on each subject who participated in the study by standard phase-encoding techniques (4.5 mm thick with 3.75 mm $\times$ 3.75 mm in-plane voxel resolution, inter-slice distance 1 mm, TR = 1600 ms, flip angle = 90°, field of view = 240 mm $\times$ 240 mm $\times$ 256 mm, interleaved slice acquisition, matrix size = 64 mm $\times$ 64 mm; 16 slices oriented along the calcarine sulcus) with the modification that two wedges of an 8 Hz flicker black and white polar checkerboard grating were bilaterally opposite like a bow tie, to enhance signal-to-noise ratio (Sereno et al 1995; Slotnick and Yantis 2003). Wedges occupied a given location for 2 TRs (3.2 s) before moving to the adjacent location in a clockwise fashion. Each wedge subtended 18 deg of 360 deg. Six TRs of dummy scans were discarded before each run to bring spins to baseline. 168 volumes were collected on each run. A minimum of 7 wedge runs were collected for each subject and then averaged to minimize noise before retinotopic data analysis in BV. A minimum of 3 runs was collected per subject with expanding 8 Hz flickering concentric rings each of which spanned approximately 1 deg in ring width.

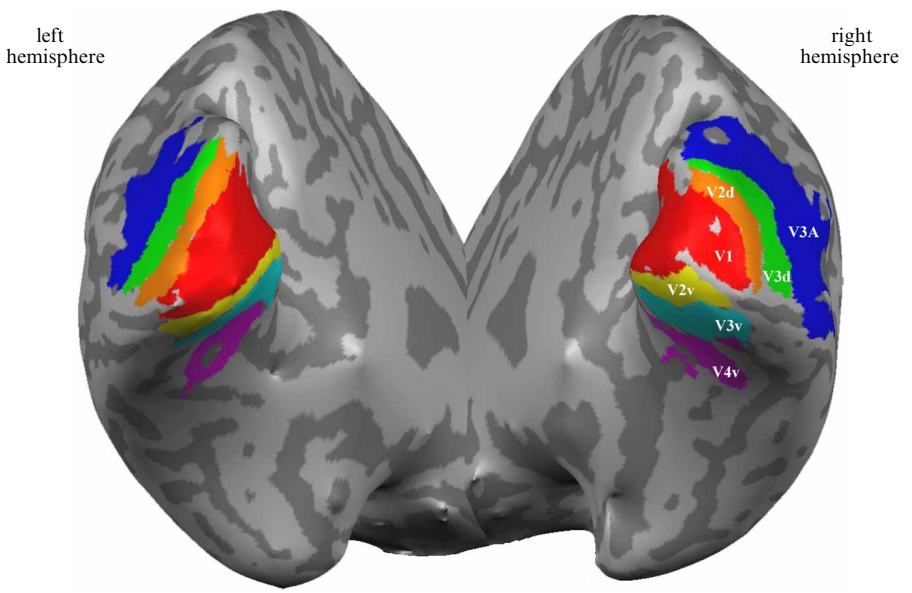

Figure 4. Retinotopic areas. Example of a single subject's right and left hemispheres with delineated retinotopic areas marked.

Each ring was updated after one TR (1.6 s), after which it was replaced by its outward neighbor, except that the outermost ring was replaced by the innermost ring, whereupon the cycle was repeated. Retinotopic areas (V1, V2d, V2v, V3d, V3v, V4v/VO1, and V3A) were defined as masks on the basis of standard criteria (Sereno et al 1995), assuming a contralateral quadrant representation for V2d, V2v, V3d, and V3v, and a contralateral hemifield representation for V1, V4v/ VO1, and V3A (Tootell et al 1997). V4v and the hemifield representation just anterior to it, called VO (Brewer et al 2005), were combined into a common mask because the border between these regions was not distinct in all subjects.

3 Results

We found angle-correlated BOLD activity in all the retinotopic visual areas of the cortex (figures 5 and 6). BOLD signal varied as a function of corner angle, with sharp corner angles driving stronger responses and shallow corner angles driving weaker responses. Figure 5 shows the average time-courses (twenty-four subjects) of the responses from all retinotopic areas tested, for the 5 different angle conditions. Time courses for the individual retinotopic areas were also obtained (supplemental figure S1, online only at http://www.perceptionweb.com/misc/p5610/). For each retinotopic area, we calculated each subject's average response to each angle condition (5 – 20 s after stimulus onset) and calculated the %BOLD signal z-score across the 5 conditions for that subject. z-scoring of the responses reduced a large fraction of the BOLD signal variation between subjects. When we plotted the %BOLD signal z-score (twenty-four subjects average) against the angle of the corner, we found a parametric relationship, both for the union of all localized retinotopic areas and for each of the individual retinotopic areas examined (figure 6). For each retinotopic area we performed a repeated-measures ANOVA with a linear contrast based on the condition angle: the amount of variance in the z-scores that is accounted for by the linear contrast (η_p^2) reached significance at a level of $p < 0.01$ in all individual areas, as well as in the union of all retinotopic areas.

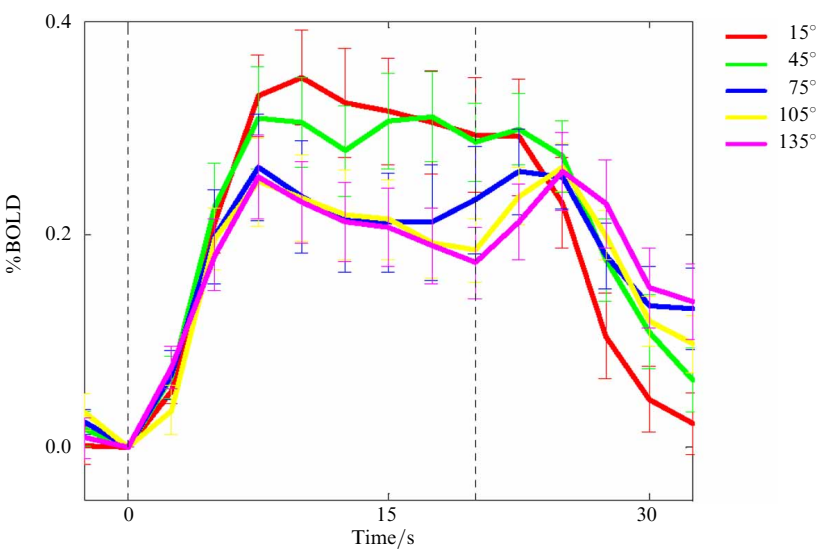

Figure 5. %BOLD responses to the ABS stimulus, from all localized retinotopic areas in twenty-four subjects. Average response time-course plots from all 5 angle conditions, color-coded for different corner angles. We used the union of all the retinotopic areas in each subject as that subject's region of interest (ROI). Dotted vertical lines indicate ABS stimulus onset and termination. Error bars represent ± 1 SEM between subjects.

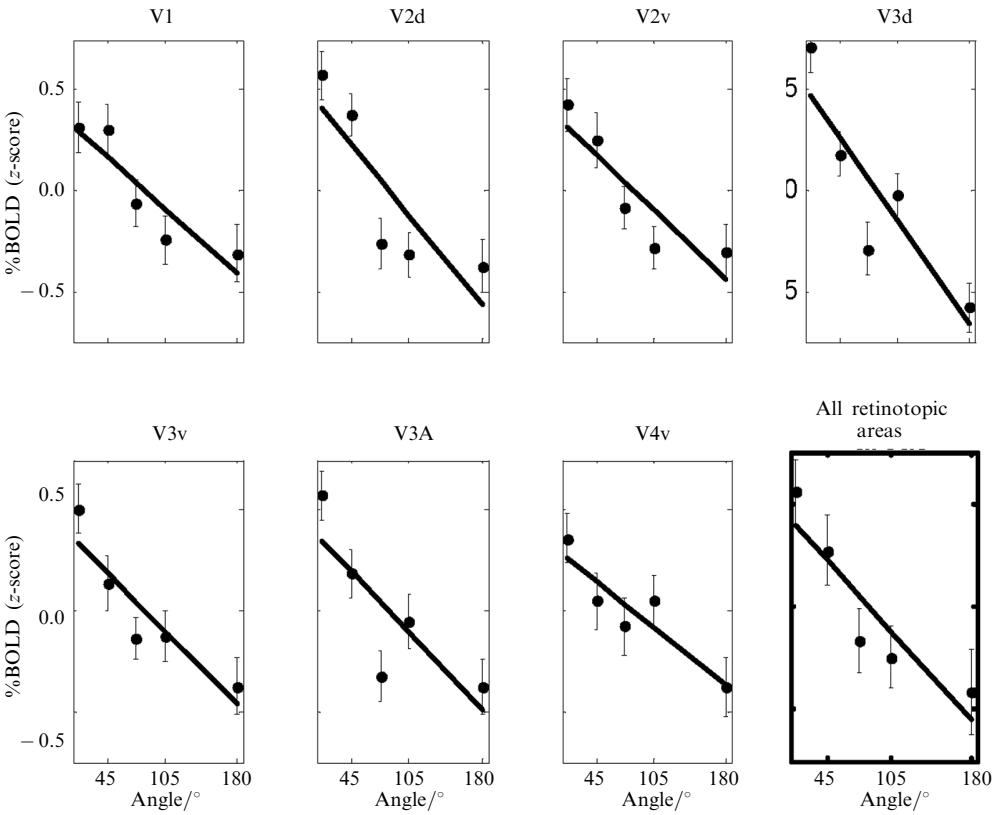

Figure 6. %BOLD signal (*z*-score) as function of corner angle, in individual retinotopic areas, as well as in the union of all localized retinotopic areas. Each data point was obtained by first averaging the responses between 5 and 20 s after stimulus onset, for each subject's hemisphere, and then computing the *z*-score across the 5 angle conditions. Regression lines were calculated with the least-squares fit. Error bars represent ± 1 SEM between subject hemispheres. The union of all localized retinotopic areas was calculated from the data in figure 5.

These results offer the first physiological correlates of the ABS illusion. Moreover, they agree with previous psychophysical measurements of this illusion (Troncoso et al 2005), and suggest that sharp corners are more powerful stimuli than shallow corners throughout the human occipital cortex.

4 Discussion

4.1 *General comments*

Certain image cues are more informative about world structure than others. According to information theory (Shannon 1948), regions in the retinal image where sudden changes occur contain more information about the spatiotemporal structure of the environment than uniform regions. Adjacent or subsequent portions of the image are unpredictable in discontinuous domains, whereas continuous regions are predictable by definition.

Werner (1935) described angles as "those parts of contour which have stored within them the greatest amount of psychophysical energy" (page 43), and proposed that "angles are especially intense parts of contour, and there is invested in them a central significance for the construction of optical figurations" (page 46). Attneave (1954) subsequently pointed out that the most informative part of a contour is a contour discontinuity. A recent study has shown that information is quantifiably higher at acute than at obtuse corners (Feldman and Singh 2005). The visual system may have evolved to be

especially sensitive to contour discontinuity, because rapid detection and processing of these cues may provide the most efficient route to recovering world structure from the image (Gibson 1950).

Curvature and corner features have been involved in numerous visual processes, such as shape analysis (Attneave 1954; Biederman 1987), texture segmentation (Rubenstein and Sagi 1996; Barth et al 1998), filling-in (Tse 2002), processing of motion signals (Loffler and Orbach 1999; Pack et al 2003; Caplovitz and Tse 2006), attentional capture (Cole et al 2001), and saccade selection (Krieger et al 2000). The prevalence and distribution of corners and curves in natural environments have also been recently determined by analysis of natural scenes (Krieger et al 2000; Sigman et al 2001; Yang and Purves 2003). Visual-search studies have found that several form-based 'features', including certain types of contour junctions (Enns and Rensink 1991), contour concavities (Hulleman et al 2000), corners (Humphreys et al 1994), contour curvature (Wolfe et al 1992) and curvature discontinuities (Kristjansson and Tse 2001) pop-out amongst a set of distractors. It is commonly believed that features that exhibit pop-out during visual search are processed rapidly and in parallel across the visual field (Treisman and Gelade 1980). Given the importance of contour discontinuities to recovering form information, it is possible that the visual system may have evolved a specialized ability to detect these key features rapidly across the image. This suggests that processing of corners and other informative contour discontinuities begins early in the visual hierarchy.

4.2 *Physiological bases of corner and curvature processing*

The physiological responses to corners, curves, and terminators have generated a great deal of interest in recent years (Pasupathy and Connor 1999, 2001, 2002; Pack and Born 2001; Pack et al 2003, 2004; Ito and Komatsu 2004; Pack et al 2004). Electrophysiological studies have reported single-unit responses to curves and corners in the striate and extrastriate cortex of cats and primates (Hubel and Wiesel 1965; Pasupathy and Connor 1999). However, many important questions remain. For instance, the neural correlates of corner processing in the human brain are unknown. Specifically, the BOLD correlates of corner perception have not been studied in any species to date. Finally, neuroimaging and electrophysiological studies have yet to determine the contribution of angle sharpness to corner processing in any species.

Here we used the ABS illusion as a tool to systematically investigate the physiological correlates of corner and angle processing in humans, through functional imaging. We found BOLD signal strength to be positively correlated with both the acuteness of corner angle and the strength of the ABS illusion, since the strength of the ABS illusion itself increases with angle acuteness. These results support earlier psychophysical data collected while presenting equivalent stimuli (Troncoso et al 2005). Just as edge-based illusions, such as Mach bands and Chevreul's effect (in which adjacent surfaces in a luminance staircase give rise to illusory brightness at the surface borders) provide information relevant to the perception of all edges, the Vasarely and the ABS effects studied here provide information that is relevant to corner perception in general.

Hurvich (1981) suggested that Vasarely's nested-squares illusion (figure 1) could be explained by contrast differences at the level of center-surround receptive fields. On the basis of this idea, Troncoso et al (2005) proposed more generally that any surface corner will increase local contrast, and so sharp corners will be perceptually more salient than shallow corners. That is, deflections or discontinuities in edges, such as corners, curvature, and terminators, may be first processed by center–surround receptive fields, as the antagonism between center and surround should result in sharp corners, curves or endpoints being more potent stimuli than shallow corners/curves, or flat edges (Troncoso et al 2005). We propose that the changes in BOLD signal observed

here are also primarily driven by changes in local contrast at the corners (as local contrast, from the point of view of a single receptive field in the early visual areas, is higher at sharp than at shallow corners).

This hypothesis is fully compatible with the involvement of later cortical stages in the further processing of corner angles. For instance, we should expect that the orientation of corner angles will be processed cortically, given that the first orientation-selective cells are cortical. Pasupathy and Connor (1999, 2001, 2002) have found that neuronal responses in area V4 are selective to specific curvature orientations and spatial locations.

Moreover, as with most physiological studies of visual perception, our results do not rule out the potential involvement of lateral cortical connections or the role of feedback (Martinez-Conde et al 1999; Girard et al 2001, 2002). Future single-unit studies will determine whether responses from neurons with center – surround receptive fields may match the perception of corners and the ABS illusion (Troncoso et al 2005). Single-unit studies will furthermore address the specific hypothesis that the physiological effects seen here are due to the interaction of corners and receptive-field organization.

Our local-contrast hypothesis is moreover consistent with previous human fMRI studies showing that increments in perceived contrast are correlated with increases in BOLD response in striate and extrastriate cortex (Boynton et al 1999). However, there have been no previous studies of the effect of varying corner angles on local contrast.

Our results also agree with previous electrophysiological studies showing that responses to corners can be found in striate and extrastriate neurons (Hubel and Wiesel 1965; Pasupathy and Connor 1999). However, we also found some intriguing differences. Electrophysiological studies in primate area V1 (Shevelev et al 1998) and area V2 (Ito and Komatsu 2004) have reported that corner-responsive neurons are tuned to specific corner angles, with all the different corner angles (whether sharp or shallow) being represented across the neuronal population (just as different cortical neurons prefer different edge orientations). In contrast, we found that neural activity within all localized retinotopic areas in the human cortex is greatest in response to sharp corner angles, as one might predict from Attneave's (1954) psychophysical observations on shape recognition and from the perceptual quantification of the ABS illusion (Troncoso et al 2005). Pasupathy and Connor (1999) showed that over 70% of the V4 neurons tuned to corner angles also respond more vigorously to sharp than to shallow angles. However, our findings were common to all cortical retinotopic areas, not just V4.

4.3 *The effect of spatial-frequency content vs local contrast on corner physiology and perception*

Here we propose that the changes in perceptual salience and correlated BOLD signal that are associated with varying corner angles are driven primarily by changes in local contrast at the corners. That is, the sharper the corner angle, the higher the local contrast at the corner (as illustrated in figures 2d and 2g) and the stronger the BOLD activation. This follows from Hurvich (1981), who proposed that local contrast processes are the basis for Vasarely's nested-squares illusion, on which the ABS is based.

An alternative (and not necessarily exclusive) hypothesis would be that the present results are driven by differences in spatial frequency, rather than by differences in local contrast, for different corner angles. We therefore measured the effects of corner angle on spatial-frequency content. Figure 7 shows a plot of the power spectrum across the different angle conditions tested in the current experiments. Although the spatial-frequency differences between angles might potentially account for the changes in BOLD observed, the current results are also consistent with previous contrast fMRI studies showing that psychophysically detected contrast increments are related to increases in BOLD in both striate and extrastriate cortex areas (Boynton et al 1999).

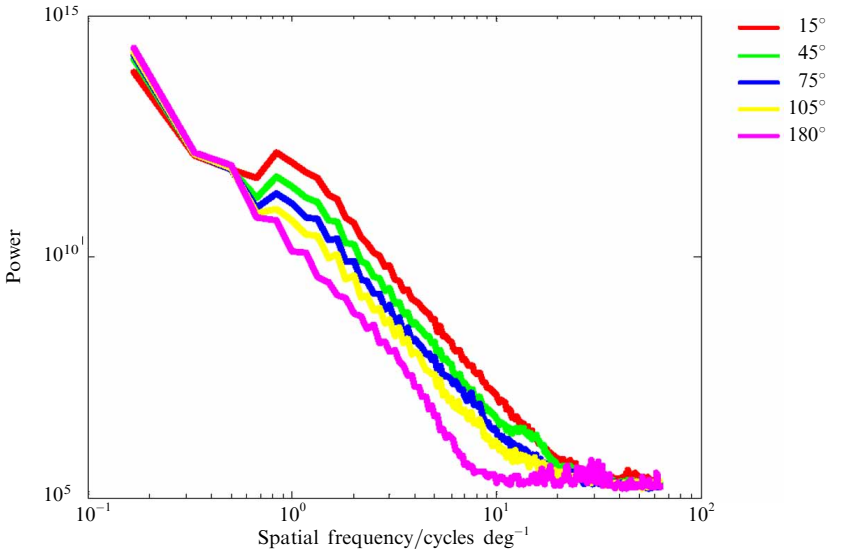

Figure 7. Spatial-frequency content of the Alternating Brightness Star illusion. Frequency power spectrum for all angle conditions in the ABS configuration used in the current fMRI experiments.

One should also note that, if future more refined analysis reveals that the current results are indeed explained by spatial-frequency content, no extant theories of corner perception suggest that corners become more salient as a function of their angle owing to spatial-frequency content. Thus, if spatial-frequency content is the ultimate reason for the corner-angle effects reported here, then the present results will have established a new role for spatial-frequency analysis by the brain.

In summary, we found that BOLD signal varied as a function of corner angle throughout the retinotopic visual cortex. The enhancement from sharp corners occurred in all localized retinotopic areas, consistent with Troncoso et al's (2005) proposal that most visual neurons will respond more strongly to sharp than to shallow corners, including neurons with center–surround receptive fields in the retina and/or the lateral geniculate nucleus (LGN). Therefore, this result rules out the possibility that all corner processing takes place in any given retinotopic cortical region (or subset of retinotopic regions).

The results provide the first physiological evidence that corner angle plays an important role in stimulus salience throughout the visual system, including stages at least as early as area V1.

Acknowledgments. We thank Shannon Bentz, Veronica Shi, Tammy Moran, and Elizabeth Do for technical assistance, and Nicole Rust and Tanya Baker for their advice on data analysis. This project was funded by a Burke Award and NIH R03 MH0609660-01 grant to PUT, by a Dana Foundation Program in Brain and Immuno-Imaging grant to SM-C, and by Barrow Neurological Foundation grants to SM-C and SLM. XGT was a fellow of the University College London Graduate School Fund.

References

Attneave F, 1954 "Some informational aspects of visual perception" *Psychological Review* **61** 183

Barth E, Zetzsche C, Rentschler I, 1998 "Intrinsic two-dimensional features as textons" *Journal of the Optical Society of America A* **15** 1723 – 1732

Biederman I, 1987 "Recognition-by-components: a theory of human image understanding" *Psychological Review* **94** 115 – 147

Boynton G M, Demb J B, Glover G H, Heeger D J, 1999 "Neuronal basis of contrast discrimination" *Vision Research* **39** 257 – 269

Brewer A A, Liu J, Wade A R, Wandell B A, 2005 "Visual field maps and stimulus selectivity in human ventral occipital cortex" *Nature Neuroscience* **8** 1102 – 1109

Caplovitz G P, Tse P U, 2006 "Mechanisms underlying the perceived angular velocity of a rigidly rotating object" *Vision Research* **46** 2877 – 2893
Cole G, Gellatly A, Blurton A, 2001 "Effect of object onset on the distribution of visual attention" *Journal of Experimental Psychology: Human Perception and Performance* **27** 1356 – 1368
Enns J T, Rensink R A, 1991 "Preattentive recovery of three-dimensional orientation from line drawings" *Psychological Review* **98** 335 – 351
Feldman J, Singh M, 2005 "Information along contours and object boundaries" *Psychological Review* **112** 243 – 252
Gibson J J, 1950 "The perception of visual surfaces" *American Journal of Psychology* **63** 367 – 384
Girard P, Hupe J M, Bullier J, 2001 "Feedforward and feedback connections between areas V1 and V2 of the monkey have similar rapid conduction velocities" *Journal of Neurophysiology* **85** 1328 – 1331
Girard P, Lomber S G, Bullier J, 2002 "Shape discrimination deficits during reversible deactivation of area V4 in the macaque monkey" *Cerebral Cortex* **12** 1146 – 1156
Hubel D H, Wiesel T N, 1965 "Receptive fields and functional architecture in two non-striate visual areas (18 and 19) of the cat" *Journal of Neurophysiology* **28** 229 – 289
Hulleman J, Winkel W te, Boselie F, 2000 "Concavities as basic features in visual search: evidence from search asymmetries" *Perception & Psychophysics* **62** 162 – 174
Humphreys G W, Keulers N, Donnelly N, 1994 "Parallel visual coding in three dimensions" *Perception* **23** 453 – 470
Hurvich L M, 1981 *Color Vision* (Sunderland, MA: Sinauer Associates)
Ito M, Komatsu H, 2004 "Representation of angles embedded within contour stimuli in area V2 of macaque monkeys" *Journal of Neuroscience* **24** 3313 – 3324
Krieger G, Rentschler I, Hauske G, Schill K, Zetzsche C, 2000 "Object and scene analysis by saccadic eye-movements: an investigation with higher-order statistics" *Spatial Vision* **13** 201 – 214
Kristjansson A, Tse P U, 2001 "Curvature discontinuities are cues for rapid shape analysis" *Perception & Psychophysics* **63** 390 – 403
Loffler G, Orbach H S, 1999 "Computing feature motion without feature detectors: a model for terminator motion without end-stopped cells" *Vision Research* **39** 859 – 871
Martinez-Conde S, Cudeiro J, Grieve K L, Rodriguez R, Rivadulla C, Acuna C, 1999 "Effects of feedback projections from area 18 layers 2/3 to area 17 layers 2/3 in the cat visual cortex" *Journal of Neurophysiology* **82** 2667 – 2675
Martinez-Conde S, Macknik S L, 2001 "Junctions are the most salient visual features in the early visual system", in *Society for Neuroscience 31st Annual Meeting* (San Diego, CA: Society for Neuroscience) online
Pack C C, Born R T, 2001 "Temporal dynamics of a neural solution to the aperture problem in visual area MT of macaque brain" *Nature* **409** 1040 – 1042
Pack C C, Gartland A J, Born R T, 2004 "Integration of contour and terminator signals in visual area MT of alert macaque" *Journal of Neuroscience* **24** 3268 – 3280
Pack C C, Livingstone M S, Duffy K R, Born R T, 2003 "End-stopping and the aperture problem: two-dimensional motion signals in macaque V1" *Neuron* **39** 671 – 680
Pasupathy A, Connor C E, 1999 "Responses to contour features in macaque area V4" *Journal of Neurophysiology* **82** 2490 – 2502
Pasupathy A, Connor C E, 2001 "Shape representation in area V4: position-specific tuning for boundary conformation" *Journal of Neurophysiology* **86** 2505 – 2519
Pasupathy A, Connor C E, 2002 "Population coding of shape in area V4" *Nature Neuroscience* **5** 1332 – 1338
Rubenstein B S, Sagi D, 1996 "Preattentive texture segmentation: the role of line terminations, size, and filter wavelength" *Perception & Psychophysics* **58** 489 – 509
Sereno M I, Dale A M, Reppas J B, Kwong K K, Belliveau J W, Brady T J, Rosen B R, Tootell R B, 1995 "Borders of multiple visual areas in humans revealed by functional magnetic resonance imaging" *Science* **268** 889 – 893
Shannon C, 1948 "A mathematical theory of communication" *The Bell System Technical Journal* **27** 379 – 423
Shevelev I A, Lazareva N A, Sharaev G A, Novikova R V, Tikhomirov A S, 1998 "Selective and invariant sensitivity to crosses and corners in cat striate neurons" *Neuroscience* **84** 713 – 721
Sigman M, Cecchi G A, Gilbert C D, Magnasco M O, 2001 "On a common circle: natural scenes and Gestalt rules" *Proceedings of the National Academy of Sciences of the USA* **98** 1935 – 1940
Slotnick S D, Yantis S, 2003 "Efficient acquisition of human retinotopic maps" *Human Brain Mapping* **18** 22 – 29

Tootell R B, Mendola J D, Hadjikhani N K, Ledden P J, Liu A K, Reppas J B, Sereno M I, Dale A M, 1997 "Functional analysis of V3A and related areas in human visual cortex" *Journal of Neuroscience* **17** 7060 – 7078

Treisman A M, Gelade G, 1980 "A feature-integration theory of attention" *Cognitive Psychology* **12** 97 – 136

Troncoso X G, Macknik S L, Martinez-Conde S, 2005 "Novel visual illusions related to Vasarely's 'nested squares' show that corner salience varies with corner angle" *Perception* **34** 409 – 420

Tse P U, 2002 "A contour propagation approach to surface filling-in and volume formation" *Psychological Review* **109** 91 – 115

Vasarely V, 1970 *Vasarely* volume II (Neuchâtel: Éditions du Griffon)

Vasarely V, 1982 *Gea* (Paris: Éditions Hervas)

Werner H, 1935 "Studies on contour: I. Qualitative analyses" *American Journal of Psychology* **47** 40 – 64

Wolfe J M, Yee A, Friedman-Hill S R, 1992 "Curvature is a basic feature for visual search tasks" *Perception* **21** 465 – 480

Yang Z, Purves D, 2003 "Image/source statistics of surfaces in natural scenes" *Network* **14** 371 – 390